ORIGINAL ARTICLE

Physiology and whole-plant carbon partitioning during stem sugar accumulation in sweet dwarf sorghum

Benjamin A. Babst[1,2] · Abhijit Karve[1,3] · Anthony Sementilli[1,4,5] · Ismail Dweikat[6] · David M. Braun[7]

Abstract

Main conclusion **A greater rate of phloem unloading and storage in the stem, not a higher rate of sugar production by photosynthesis or sugar export from leaves, is the main factor that results in sugar accumulation in sweet dwarf sorghum compared to grain sorghum.**

Abstract At maturity, the stem internodes of sweet sorghum varieties accumulate high concentrations of fermentable sugars and represent an efficient feedstock for bioethanol production. Although stem sugar accumulation is a heritable trait, additional factors that drive sugar accumulation in sorghum have not been identified. To identify the constraints on stem sugar accumulation in sweet sorghum, we used a combination of carbon-11 (^{11}C) radiotracer, physiological and biochemical approaches, and compared a grain sorghum and sweet dwarf sorghum line that have similar growth characteristics including height. Photosynthesis did not increase during development or differ between the sorghum lines. During the developmental transition to the reproductive stage, export of ^{11}C from leaves approximately doubled in both sorghum lines, but ^{11}C export in the sweet dwarf line did not exceed that of the grain sorghum. Defoliation to manipulate relative sink demand did not result in increased photosynthetic rates, indicating that the combined accumulation of C by all sink tissues was limited by the maximum photosynthetic capacity of source leaves. Nearly 3/4 of the ^{11}C exported from leaves was transported to the lower stem in sweet sorghum within 2 h, whereas in grain sorghum nearly 3/4 of the ^{11}C was in the panicle. Accordingly, the transcripts of several sucrose transporter (SUT) genes were more abundant in the stem internodes of the sweet dwarf line compared to the grain sorghum. Overall, these results indicate that sugar accumulation in sweet sorghum stems is influenced by the interplay of different sink tissues for the same sugars, but is likely driven by elevated sugar phloem unloading and uptake capacity in mature stem internodes.

Keywords Sweet sorghum · Sucrose accumulation · Carbon-11 partitioning · Phloem unloading

---

Communicated by Anastasios Melis.

S.I.: Sorghum.

✉ Benjamin A. Babst
babst@uamont.edu

1 Biological, Environmental and Climate Sciences Department, Brookhaven National Laboratory, Upton, NY 11973-5000, USA

2 Present Address: Arkansas Forest Resources Center, and College of Forestry, Ag. and Natural Resources, University of Arkansas at Monticello, Monticello, AR 71656, USA

3 Present Address: Purdue Research Foundation, West Lafayette, IN 47906, USA

4 Department of Physical Sciences, St Joseph's College, Patchogue, NY 11772, USA

5 Present Address: Department of Chemistry and Chemical Biology, Cornell University, Ithaca, NY 14853, USA

6 Department of Agronomy and Horticulture, University of Nebraska-Lincoln, Lincoln, NE 68583-0915, USA

7 Divisions of Plant and Biological Sciences, University of Missouri, Columbia, MO 65211, USA

Introduction

Accumulation of soluble carbohydrates in stem internodes of "sweet" varieties of sorghum (*Sorghum bicolor*) is valuable for sorghum syrup production, and it also has great potential as a bioenergy feedstock (Dweikat et al. 2012; Gelli et al. 2016; Rooney et al. 2007; Bihmidine et al. 2013). Like sugarcane, the soluble sugars can be pressed from high biomass sweet sorghum stems as a syrup, which can be directly fermented without the energy-intensive processing necessary to liberate sugars from lignocellulosic materials (Bryan 1990; Prasad et al. 2007). Unlike sugarcane, sorghum can be grown in temperate climates, and has lower water and nutrient requirements (Calvino and Messing 2012; Murray et al. 2008; Olson et al. 2013; Rooney et al. 2007).

The sugars accumulated in sorghum stems originate in leaves, derived from the products of photosynthesis. Studies of sugarcane indicate that the capacity of stems to take up sugars can be a limiting factor in some conditions, rather than the photosynthetic capacity of leaves (McCormick et al. 2006, 2008). It is not clear that sugarcane is sink limited in all conditions, or whether sink limitation may occur in sorghum also.

Like all aspects of plant growth, development and yield, transport of sugars produced in leaves is crucial to sugar accumulation. Sugars are transported from leaves to other parts of the plant by bulk flow through the phloem (Rennie and Turgeon 2009; Knoblauch and Peters 2010). Sucrose is the primary transport sugar in sorghum and that sucrose is loaded into the phloem through an apoplastic pathway (Bihmidine et al. 2015; Milne et al. 2013), as in the closely related *Zea mays* (Babst et al. 2013; Lohaus et al. 2000; Ohshima et al. 1990; Weiner et al. 1991; Slewinski et al. 2009, 2010). Export of sucrose from the leaf may be controlled by biochemical partitioning of carbon to glucose, starch and sucrose within the leaf, by efflux of sucrose into the apoplast by SWEET transmembrane channels, and by uptake from the apoplast into companion cells by sucrose transporters (SUTs) (Babst et al. 2013; Slewinski and Braun 2010; Bihmidine et al. 2015, 2016; Baker et al. 2016; Bezrutczyk et al. 2018). These controls on phloem loading could possibly be choke points for the transport and accumulation of sucrose in stems.

In addition to carbon export from source leaves, phloem unloading can be a crucial determinant of carbon partitioning (Lacointe and Minchin 2008). Unloading of sugars from the phloem may involve either apoplastic or symplastic pathways (Bihmidine et al. 2013; Patrick 2013; Ross-Elliott et al. 2017), and may change during different developmental stages (Viola et al. 2001). In sweet sorghum stems, *SUT* gene expression and dye transport assays indicate an apoplastic unloading pathway at the sugar accumulating stage (Bihmidine et al. 2015). Thus, the accumulation of sugars in sweet sorghum stems could be limited by photosynthetic capacity, export of sugars from leaves through the phloem, and the capacity to unload sucrose from the phloem, and/or store it in storage tissues in the stem.

Here, we compare one sweet and one grain sorghum line to elucidate the basis for the differences in carbon partitioning between these two varieties of the same species. While sweet sorghum varieties accumulate soluble sugars to high concentrations at maturity, grain varieties generally do not, instead channeling carbohydrates toward starch accumulation in the panicle. One challenge in comparing grain and sweet sorghum lines is that grain sorghum varieties typically have been bred for dwarf phenotypes to avoid lodging due to the weight of the large panicle, and so are much shorter than sweet sorghum lines and typically begin anthesis earlier. To isolate differences in carbon partitioning that are relevant to sugar accumulation rather than stem elongation, we used an early maturing "sweet dwarf" sorghum line (Gorz et al. 1990). Another long-standing challenge to studying carbon partitioning has been limited availability of technology to measure instantaneous or short-term rates of carbon partitioning. We fed carbon-11 (^{11}C) to leaves as $^{11}CO_2$, and used gamma detectors and positron emission tomography (PET) imaging to measure carbon partitioning in grain and sweet dwarf sorghum varieties over the course of development. Together with physiological, biochemical, and molecular assays, we tested whether stem sugar accumulation is driven by increased photosynthetic rates in source leaves, increased phloem loading and export of carbon from leaves, or phloem unloading into sink tissues, which provided insights into the control of sugar accumulation in this important biofuel crop.

Materials and methods

Plant material and growth conditions

The sweet dwarf sorghum line, N98 (PI 535783), used in this study was the result of multiple crosses of AN39, (N4692-Rio)4, 'Waconia' sweet sorghum, and 'Fremont' forage sorghum parentage to generate sweet sorghum lines with shorter time to maturity (Gorz et al. 1990). Seeds of grain sorghum (Macia), and sweet dwarf sorghum (N98) were soaked overnight in deionized water and sown in potting mix (2:1:1, Promix BX™:sand:perlite) supplemented with 16 g of Osmocote® Plus (15:9:12, N:P:K) in 14.9 L pots. The plants were grown in a greenhouse maintained at 16 h photoperiod with supplemental HID lighting in the morning and at night, and 30/24 °C day/night temperature. To acclimate the plants to the conditions of the $^{11}CO_2$ labeling

chamber, the greenhouse-grown plants were transferred to a Conviron® growth chamber maintained at 28/22 °C day/night temperature cycle, 50% RH and 600 µmol m^{-2} s^{-1} of light intensity 4 d before $^{11}CO_2$ labeling. Plant heights were measured from the soil surface to the uppermost visible leaf collar. Stem diameters were measured using calipers at 5 cm above the soil surface. For dry biomass, we separated plant leaf, stem, seedhead, and root tissues (cleaned of soil matter) and dried them at 60 °C until tissues no longer decreased in mass between measurements on subsequent days (about 1 week).

$^{11}CO_2$ administration

To study the changes through development, carbon partitioning was measured in sorghum plants using $^{11}CO_2$ from 28 days after planting (DAP) (early vegetative, 5 leaf stage) through 110 DAP (grain filling stage). $^{11}CO_2$ was produced using an EBCO T19 cyclotron by $^{14}N(p,\alpha)^{11}C$ nuclear transformation (Ferrieri and Wolf 1983) and was captured on either a stationary or portable molecular sieve trap as previously described (Babst et al. 2013; Karve et al. 2015; Kim et al. 2014). To administer the tracer, the trap was heated to 350 °C to release the $^{11}CO_2$ as a 1 min pulse in a continuous airflow, with a flow rate of 0.02 L min^{-1}, to a single leaf in a 0.06 L leaf cuvette lit by red–blue LED arrays, with light intensity of 800 µmol m^{-2} s^{-1}. The photosynthetic leaves fixed a proportion of the $^{11}CO_2$ administered, incorporating the ^{11}C into a variety of biochemicals (e.g., sugars, starch, amino acids, lipids, etc.) together termed "photoassimilate." A proportion of the ^{11}C-labeled photoassimilate was exported from the leaf via the phloem to other parts of the plant. A radiation detector attached to the leaf cuvette allowed measurement of the amount of ^{11}C administered, and the proportion of the ^{11}C that was fixed by the leaf ("^{11}C-fixation").

Whole-plant carbon partitioning

After 2 h, we measured the partitioning of recently fixed carbon to different parts of the grain and sweet sorghum plants. Younger plants (28–63 DAP) were dissected and measured by direct radioactivity counting using a NaI scintillation detector with a large field of view on a sample container positioned with a fixed distance from the detector window to minimize geometry effects. The detector was calibrated by measuring samples of known radioactivity placed in the fixed geometry sample container. For direct radioactivity counting, the plant was dissected into, (1) the load leaf—defined as the leaf to which $^{11}CO_2$ was fed, (2) the subtending internode—the internode with direct vascular connections to the load leaf, (3) the lower stem—the part of the culm below the subtending internode after removing

the attached leaf sheaths, (4) the apex—the part of the plant above the subtending internode including the young developing leaves, and (5) the rest of the leaves—all leaves other than the load leaf and the young developing leaves. Direct radioactivity counting of the roots in situ or by first washing the roots was not possible, due to the magnitude of geometry effects of roots distributed throughout the large pot, and the time constraints of the ^{11}C half-life. For analysis of ^{11}C-partitioning in mature plants (70–110 DAP), which were too large for the direct radioactivity counting method, the entire plant was scanned in an HR + PET scanner (Siemens, Germany) operated by ECAT software (version 7.2.2) in 15 cm segments, as previously described (Karve et al. 2015). Prior to $^{11}CO_2$ administration, an automated transmission scan was performed on each segment for 4 min, whereby radioactive rods (^{68}Ge) within the PET scanner ring were sequentially exposed to measure and correct for plant tissue and soil attenuation of radioactivity in a spatially explicit manner. At 2 h following $^{11}CO_2$ administration, each 15 cm segment was scanned for 4 min to measure radioactive emissions from ^{11}C in the plant. At the end of the whole-plant scan, a 3-D image of ^{11}C distribution was reconstructed showing the total counts corrected for decay and for tissue attenuation using ECAT software (version 7.2.2). The 3-D images were analyzed using Amide software (ver. 1.0.4; http://amide.sourceforge.net/) (Loening and Gambhir 2003), by drawing a region of interest in the 3-D image around the load leaf, subtending internode, lower stem, apex and roots (see Fig. 5a). The activity from the rest of the leaves was determined by subtracting the sum of the load leaf, subtending internode, lower stem, apex, and root activity from the total plant radioactivity. All the data were decay corrected back to the time $^{11}CO_2$ was pulse administered to the load leaf and partitioning expressed as percent of the total activity exported from the load leaf.

Measurement of sugars

Soluble sucrose, glucose and fructose were extracted and analyzed as described (Babst et al. 2013). Plant tissues were frozen in liquid nitrogen and ground to a fine powder using a stainless steel ball mill (MM400, Retsch Inc., Newtown, PA, USA). Approximately, 100 mg of frozen homogenized tissue powder was weighed, and extracted in cold 75% methanol (400 µl per 100 mg) in an ice-cold ultrasonication bath for 10 min. Samples were centrifuged at 16,000 × g for 2 min to pellet plant tissue residue and 1 µL of each supernatant was spotted onto 10 cm NH$_2$-bonded silica high performance thin-layer chromatography (HPTLC) using a Linomat 5 semi-automatic precision applicator (Camag Scientific Inc., Wilmington, NC, USA). Sugars were separated on the HPTLC plates using a 75%:25% acetonitrile:H$_2$O solvent system, heat-activated at 200 °C for 10 min, and

photographed under long-wave UV irradiance to quantify the concentrations of glucose (Rf: 0.23), fructose (Rf: 0.28), and sucrose (Rf: 0.17). Each plate included authentic sugar standards at five different concentrations for a calibration curve. Images of developed HPTLC plates were imported and analyzed in ImageQuant TL 1D software (Ver. 7.0, GE Healthcare Biosciences Corp, Pittsburgh, PA, USA) and sugar concentrations determined as the amount of sugar per gram of fresh tissue mass.

Photosynthetic gas exchange

For the defoliation experiment, the maximum photosynthetic rate was measured for the third fully expanded leaf of 60–70 DAP plants immediately before defoliation, and again 1, 4, and 7 days after defoliation. The defoliation treatment comprised removing all leaf blades with a sharp razor except the third fully expanded leaf, similar to Vietor and Miller (1990). Maximum photosynthetic rate was measured using a Li-Cor 6400XT with PAR set to 2000 µmol m^{-2} s^{-1}, block temperature at 30 °C, which was very close to the greenhouse temperature, reference CO_2 at 600 ppm, and flow rate of 250 µmol s^{-1}. The cuvette was clamped midway along the leaf, avoiding the midrib for 10–15 min until the photosynthetic rate was stable for several minutes. Additionally, A/C_i curves were generated for the leaf with direct vascular connections to internode 8, which accumulated the highest sugar concentrations, in 40–50 DAP (vegetative stage) and 70–80 DAP (reproductive stage) plants. Reference CO_2 was varied, while PAR was set to 2000 µmol m^{-2} s^{-1}, RH to about 50%, and flow to 500 µmol sec^{-1}.

RNA extraction and qPCR analysis

Stem tissues of reproductive stage plants were flash frozen in liquid nitrogen, ground to fine powder, and stored at -80 °C. Total RNA was extracted from internode tissues using a Spectrum™ Plant Total RNA Extraction Kit (Sigma-Aldrich, St. Louis, MO, USA). On-column DNase I treatment (Sigma-Aldrich) was performed according to the manufacturer's protocol to remove genomic DNA contamination. The cDNA synthesis was carried out with 500 ng of RNA using a M-MuLV first strand synthesis system (New England Biolabs, Ipswich, MA, USA). Quantitative PCR amplification reactions were carried out using iQ™ SYBR® Green Supermix with ROX (Bio-Rad, Hercules, CA, USA) according to instructions provided, except being scaled down to 15 µL total reaction volume. PCR amplification reactions were performed in triplicate for each gene-specific primer pair (Supplemental Table 1) under the following temperature program: 95 °C for 10 min, 40 cycles of 95 °C for 15 s, 60 °C for 25 s and 72 °C for 30 s, followed by a melting curve for reaction validation. Gene expression was normalized by the endogenous control gene, *Sorghum bicolour EF1α* (*SbEF1α*; Qazi et al. 2012). The forward and reverse primers used in the qPCR were designed using Primer3 Express (Rozen and Skaletsky 1999). All PCR amplification reactions were performed on the RNA extracted from the tissue of three biological replicates. Relative mRNA abundance was calculated using the Pfaffl method (Pfaffl 2001). Three technical replicates were assayed for each cDNA sample and the values averaged. The efficiency of each primer pair was assessed by the use of a template dilution series. Results are expressed as relative expression values (i.e., >1 represent upregulation relative to the reference group and values <1 represent downregulation relative to the reference group).

For all experiments, statistical significance was assessed using unpaired Student's t test to compare results for the grain vs. sweet dwarf sorghum at the $p \leq 0.05$ level, $n = 3$ for most data sets unless otherwise noted in the figure captions. For morphological data, $n = 10$.

Results

A sweet dwarf sorghum line was selected to minimize the plant growth differences between the grain and sweet lines used in this study, except for sugar accumulation in the stem. The most notable morphological difference was the seed-head dry mass, which was three to four times higher in grain than sweet dwarf sorghum (Fig. 1). There were some other minor differences that appeared during later growth stages between the sweet dwarf and grain lines, such as slightly more leaves and slightly lower root biomass in grain than sweet dwarf sorghum (Fig. 1). Flowering began at 56 days after planting for grain sorghum, and about 1 week later at 63 days after planting for sweet dwarf sorghum, based on flag leaf formation and dissection to observe reproductive structures, which initially form at the shoot apex within the sheaths of the youngest leaves before emerging. Otherwise, the grain and sweet dwarf sorghum plants were similar in height, stem diameter, and shoot dry weight (Fig. 1).

Sugar accumulation in sorghum internodes coincided with the initiation of flowering. During the vegetative stage (42 days after planting), the sugar content of the middle internode 8 did not differ between grain and sweet dwarf sorghum (Fig. 2). As the plants transitioned from the vegetative to the reproductive stage (56–110 days after planting), the sugar content of these internodes increased about threefold and sixfold compared to the vegetative levels, in grain and sweet dwarf sorghum, respectively (Fig. 2a). In the sweet dwarf line, sugar concentrations were generally elevated the most in the middle internodes, and to a lesser extent in the lower internodes (Fig. 2b).
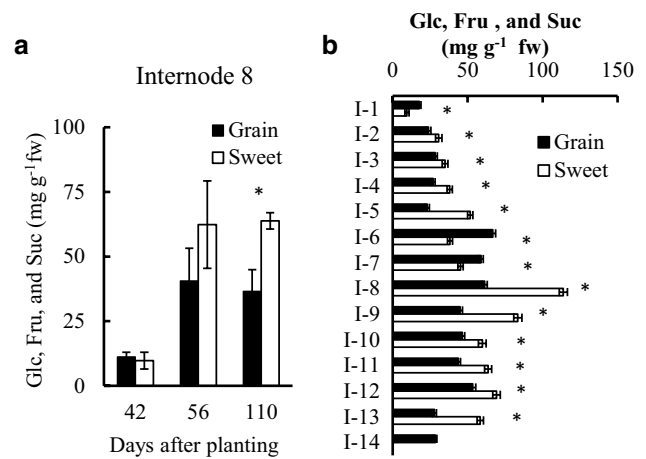
We tested the possibility that sugar accumulation is due to an increased rate of photosynthesis or increased export
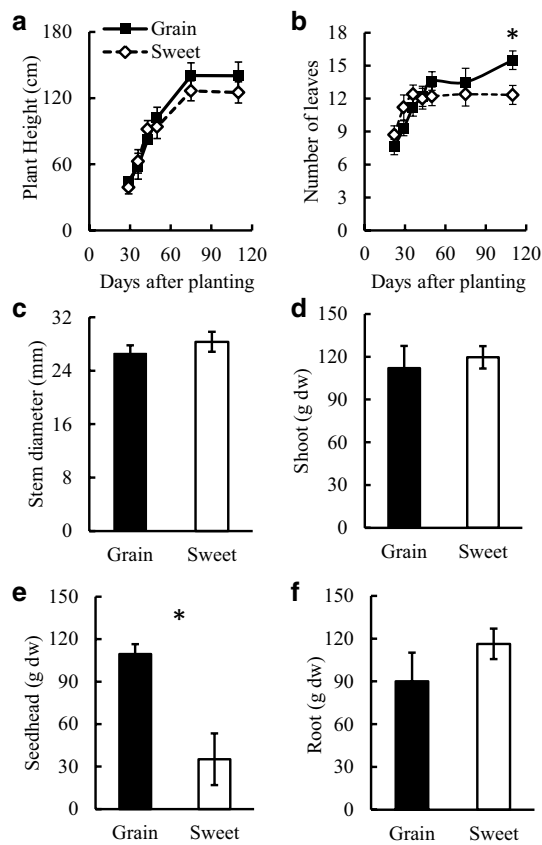
Fig. 1 The morphological character of the two lines used in this study, grain sorghum (grain) and sweet dwarf sorghum (sweet). Changes in plant height (**a**) and the number of leaves (**b**) throughout plant development from 30 DAP (4-leaf stage) to physiological maturity (120 d). Comparison of stem diameter at the base (**c**) and biomass allocation to shoots (nonreproductive parts) (**d**), seedheads (**e**), and roots (**f**) at final harvest. For all, bars indicate mean $\pm$ SE; $n = 10$

Fig. 2 Sugar profile of sorghum internodes. **a** Changes in the sugar concentration (glucose, fructose, and sucrose combined) on a fresh weight (fw) basis of the highest sugar accumulating internode (I8) before and during the vegetative stage transition of sorghum plants. **b** Concentration of soluble sugars (glc, fru and suc) at 100 DAP, during the grain filling stage. The axes are oriented such that the youngest internode is at the top of the graph, and the oldest internode is at the bottom. Internodes are numbered basipetally, starting with the internode (I-1) that was subtending the youngest leaf at the top of plant, and increasing with age. Error bars are SE, and $n = 3$ samples. Asterisks indicate statistically significant differences between grain and sweet sorghum within a time point according to a two-tailed t test

rate of photoassimilate from leaves in sweet dwarf sorghum. Photosynthesis in the sweet dwarf line was not higher than in grain sorghum across a range of internal CO_2 (C_i) concentrations either at the vegetative or reproductive stages (Fig. 3a and b, respectively). Fixation of $^{11}CO_2$, fed as a 30 s. pulse to leaves, declined late in the reproductive stage, perhaps reflecting the progression of leaf senescence at this late stage, but again did not differ between genotypes (Fig. 3c). The proportional export of ^{11}C-labeled photoassimilate from leaves increased during development (Fig. 3d). This increased export occurred slightly earlier in grain sorghum than sweet dwarf sorghum, which corresponded with the slightly earlier onset of reproductive development in the grain sorghum line. Notably, however, the C-export rate was not higher in sweet dwarf sorghum than grain sorghum during the sugar accumulation stage (70–110 days after planting).

To determine whether the sorghum lines were limited by sink demand or source capacity, we removed leaves from

sorghum plants to increase the relative ratio of sink-to-source tissue and measured the photosynthetic response. The photosynthetic rates changed slightly day-to-day similarly for both genotypes during the experiment, presumably due to slight changes in the greenhouse microclimate (Fig. 4a, b). Upon defoliation, we found a transient dip in photosynthetic rates in the remaining leaf relative to the same leaf position on control plants (Fig. 4). This type of decrease in photosynthesis has been reported previously in other species and may be a stress-type response to foliar damage (Nabity et al. 2009). However, within 4 days following defoliation, photosynthesis in the defoliated plants had quickly recovered to similar rates as control plants in both grain and sweet dwarf sorghum and remained similar 1 week after defoliation (Fig. 4).

Since photosynthetic carbon assimilation and export of assimilated carbon did not differ between grain and sweet dwarf sorghum, we tested whether the difference in sugar accumulation might be due to differences in partitioning of photoassimilates throughout the plant. Two hours after feeding $^{11}CO_2$, ^{11}C distribution throughout the plant was measured. In all stages, very little ^{11}C-photoassimilate (<0.001%) was translocated to other mature leaves (Fig. 5a), indicating that these other leaves were photosynthetically self-sufficient and were not importing photoassimilate from the labeled leaf. Increased ^{11}C export from the source leaf during the reproductive stage in both sorghum lines was reflected by
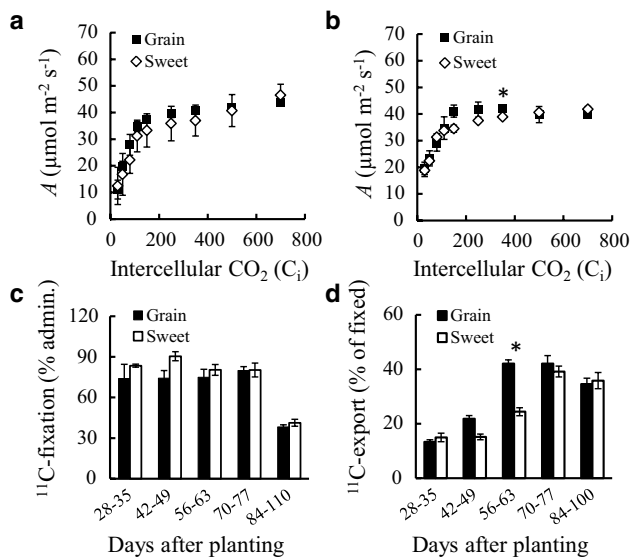
Fig. 3 Photosynthetic rates and photoassimilate export from leaves is similar in sweet dwarf and grain sorghum. Net CO_2 assimilation (A) is shown as a function of intercellular CO_2 concentration (C_i). A/C_i curves were generated for the source leaf of node 8 (attached directly to internode with the highest sugar accumulation) at the vegetative stage (**a** 40–50 DAP) and after initiation of flowering (**b** 70–80 DAP). Fixation of $^{11}CO_2$ as a percent of ^{11}C administered to the youngest fully expanded leaf (**c**) and percentage of the ^{11}C-photoassimilate translocated from the leaf to other parts of the plant (**d**) in grain and sweet dwarf sorghum. The $^{11}CO_2$ was administered as a 30 s pulse of approximately 2.8 GBq $^{11}CO_2$ in a constant stream of air through a photosynthesis cuvette. After 2 h, the labeled leaf was harvested and the activity in this leaf and the rest of the plant was measured either by a gamma counter (28–63 DAP) or by scanning the plant with a PET camera (70–110 DAP). Error bars are SE ($n = 3–4$ plants)

a decrease in ^{11}C remaining in the source leaf at the end of the 2 h period (Fig. 5b). Partitioning of ^{11}C to the internode subtending the labeled leaf increased and remained high in sweet dwarf sorghum throughout the reproductive stage, but increased only transiently in grain sorghum at the onset of the reproductive stage (Fig. 5d). The pattern of increasing ^{11}C partitioning to the lower stem was similar to the subtending internode, although the differences between grain and sweet dwarf sorghum were less pronounced (Fig. 5e). Combined, the subtending internode and lower stem accounted for about 3/4 of all ^{11}C exported from the sweet dwarf leaf. We were not able to measure partitioning to roots in young plants, but in mature reproductive plants, the sweet dwarf line partitioned a higher proportion of ^{11}C to roots ($6.5 \pm 0.073\%$) than did the grain sorghum line ($0.05 \pm 0.0001\%$). In contrast, ^{11}C partitioning to the apex reached higher levels in grain sorghum than in sweet dwarf sorghum, especially during the reproductive stage when 3/4 of all ^{11}C exported from grain sorghum leaves was found in the seedhead (Fig. 5c). Since ^{11}C export from grain and sweet dwarf sorghum source leaves was similar,
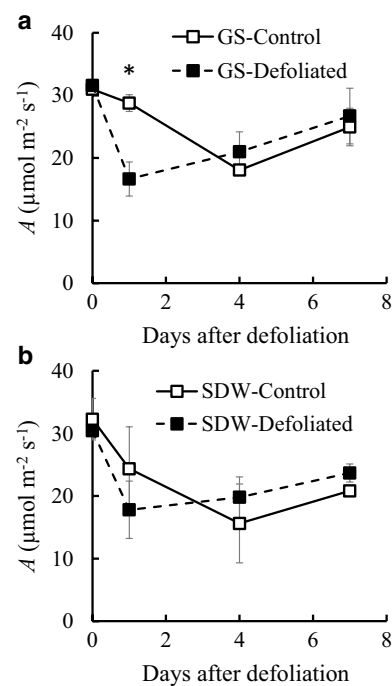
Fig. 4 Sorghum plants were source-limited. Effect of defoliation treatment on photosynthetic CO_2 assimilation of grain (**a**) and sweet dwarf sorghum (**b**). For defoliated plants, all leaves except the third fully expanded leaf were removed using a razor blade. Plants were 60–70 DAP on the day of defoliation. Bars are mean $\pm$ SE ($n = 2–4$ plants)

sugar accumulation in sweet dwarf sorghum appears to be driven not by changes in the total supply of sugars from the leaves (Fig. 3d), but by differences in the partitioning of those sugars between different sink tissues (Fig. 5).

Since sucrose is the main form of carbon transported in the phloem, is unloaded apoplastically in maturing stems, and is stored in stem parenchyma cells of sorghum (Babst et al. 2013; Bihmidine et al. 2015), we examined expression during sugar accumulation of sucrose transporters (SUTs), which are directly implicated in sucrose uptake into cells, as well as several homologs of genes that were sugar-responsive in sugarcane (Papini-Terzi et al. 2009). In our sorghum plants, expression levels of SbSUT1, SbSUT2, SbSUT4, and SbSUT6 were elevated in sweet dwarf internodes compared to grain sorghum internodes (Fig. 6). Sugar accumulation was highest in the middle and lower internodes (Fig. 2b), which is also where SbSUT1, SbSUT4, and SbSUT6 expression was elevated. There was no expression of SbSUT3 detected, as in previous studies (Bihmidine et al. 2015; Milne et al. 2017). Expression of several sugar-responsive genes was similar to expression of homologs previously reported in sugarcane (Papini-Terzi et al. 2009). Expression of SbMYB3-like and SbSnRK1 in sweet dwarf sorghum sugar-accumulating internodes was low compared to grain sorghum internodes (Fig. 6f, g). On the contrary,
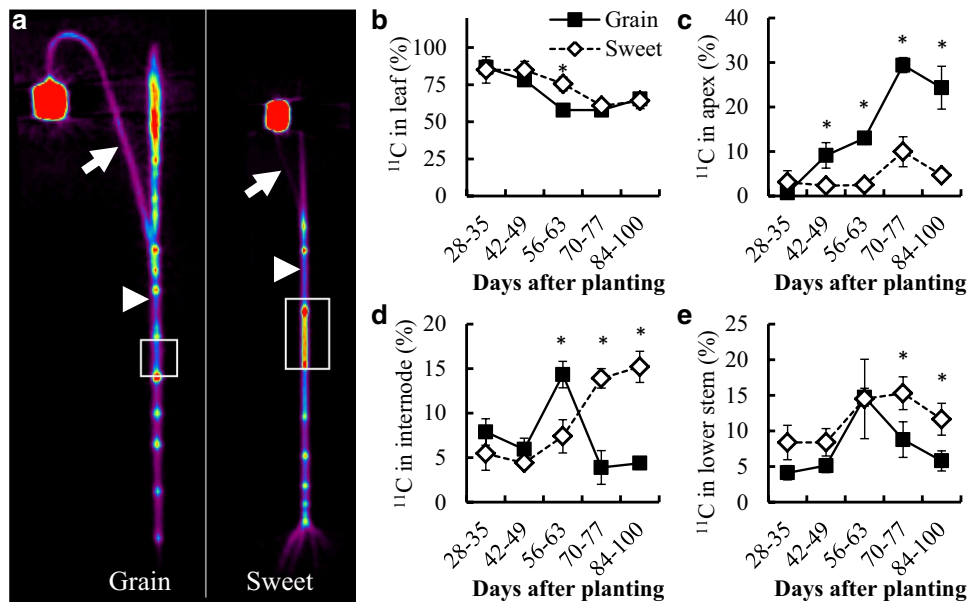
Fig. 5 Partitioning of ^{11}C-photoassimilate to different plant tissues as a percentage of the total ^{11}C fixed by the labeled leaf. (**a**) Representative PET images of ^{11}C-photoassimilate partitioning 2 h after ^{11}CO$_2$ was fed to a single leaf of grain and sweet dwarf sorghum plants. Symbols: labeled leaf blade (arrow), labeled leaf sheath (arrow head), internode below leaf sheath vascular connections to the stem (white box). Red color indicates high radioactivity from ^{11}C, while blue and black indicate low radioactivity. ^{11}C Partitioning is shown for (**b**) the leaf fed ^{11}CO$_2$, (**c**) the stem above where the labeled leaf attached to the stem (apex), (**d**) the subtending internode directly connected to the pulsed leaf, and (**e**) all internodes below the labeled leaf (lower stem). Each data point is an average of three to four plants measured over the period of that week. Error bars are SE. Asterisks indicate statistically significant differences between grain and sweet sorghum within a time point according to a two-tailed *t* test

the expression of SbMAPK4 was uniformly high in sweet sorghum, but progressively lower in the middle and upper internodes of grain sorghum (Fig. 6h).

Discussion

The fact that photosynthetic rates were similar between grain and sweet dwarf sorghum suggests that stem sugar accumulation is not driven by altered photosynthetic rates. Increasing the sink demand relative to source leaves by defoliation did not result in increased photosynthesis in either grain or sweet dwarf sorghum. In sugarcane, this defoliation approach indicated that increasing the relative sink demand may upregulate CO$_2$ assimilation in the source leaves, implying that the source leaves are not already operating at maximum capacity in some circumstances (McCormick et al. 2006, 2008). At least under the conditions of our study, both the grain and sweet dwarf sorghum lines appeared to be limited by source leaf photosynthetic capacity, not by sink uptake of photoassimilates. Hence, a mechanism other than altered photosynthetic rates must be responsible for sugar accumulation in sweet sorghum.

In both sorghum lines, we observed an increase in the proportion of fixed carbon that was exported from sorghum

leaves during the transition from the vegetative to the reproductive stage. Changes in sugar export are likely mediated by the SWEETs and SUTs that are involved in phloem loading (Bihmidine et al. 2016), although SUT expression in mature leaves was reported to be similar at the vegetative and reproductive stages (Milne et al. 2013). Coinciding with the increased carbon export, there was a transient spike in carbon partitioning to grain sorghum stems at the onset of reproduction. This is consistent with the transient accumulation of carbohydrates in stems of other monocot grain crops, such as wheat, during the transition to the reproductive stage (Scofield et al. 2009). Although transient carbohydrate accumulation could result from a change in metabolism within the stem favoring carbohydrate storage over utilization, our data suggest that increased photoassimilate export from leaves makes an important contribution. However, increased export was not the cause of the sustained sugar accumulation in sweet dwarf sorghum, because the export of carbon from leaves was no greater in sweet dwarf sorghum than in grain sorghum.

Instead, sugar accumulation in sweet sorghum internodes appears to be dependent on processes within the stem that determine photoassimilate partitioning among the different sink tissues (e.g., stems and reproductive structures). At a whole-plant level, photoassimilate partitioning may be

Fig. 6 Expression of sucrose transporters and homologs of sucrose-responsive genes in stem internodes of grain and sweet sorghum. Relative expression of SbSUT1 (**a**), SbSUT2 (**b**), SbSUT4 (**c**), SbSUT5 (**d**), SbSUT6 (**e**), SbSnRK1 (**f**), SbMYB3-like (**g**), and SbMAPK4 (**h**) were measured by qPCR in the upper, middle, and lower internodes. Bars are means ± SE; $n = 3$
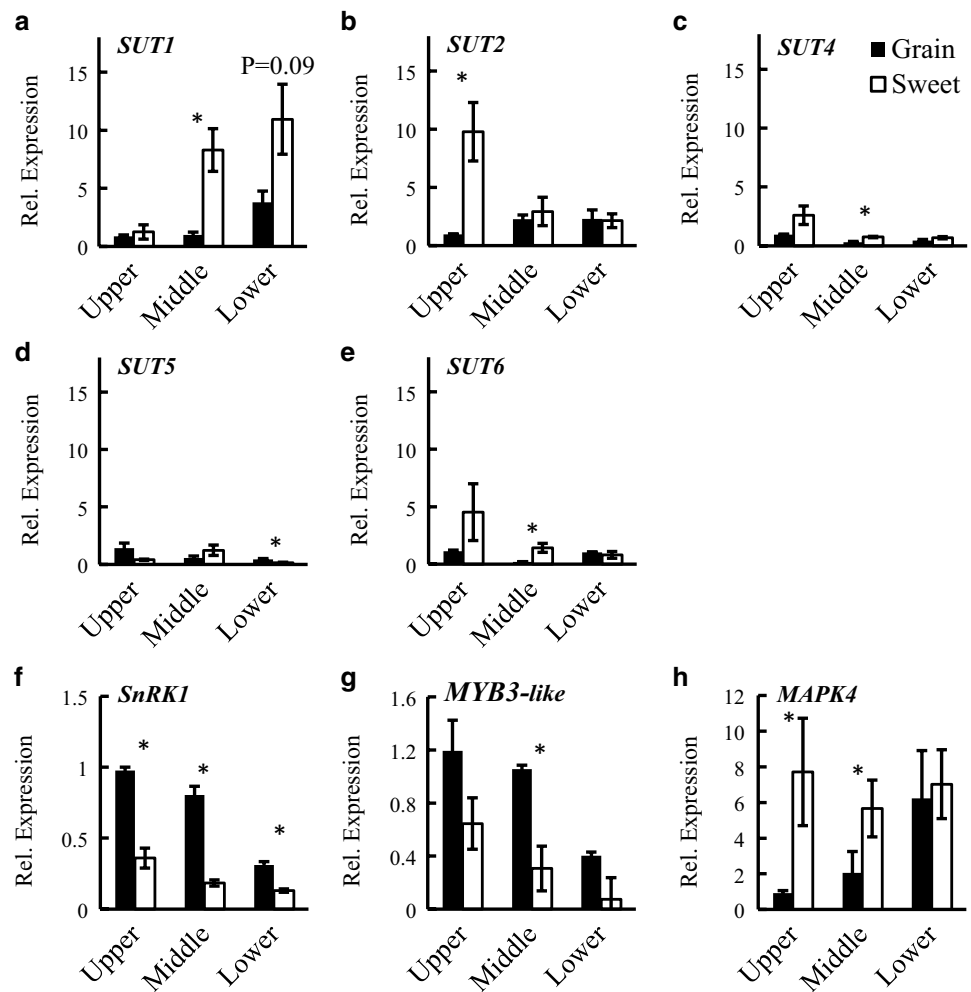
determined by differences in demand between multiple competing sinks (Lacointe and Minchin 2008; Minchin 2007). By this model, sugar accumulation in stems could be driven by increased capacity for uptake into stem storage tissues, but it is also possible that decreased demand in other sink tissues could result in greater sugar availability for stem tissues to take up. The other major sinks in sorghum at the sugar accumulating stage are the roots and seedheads. The roots had slightly higher ^{11}C partitioning in dwarf sweet sorghum, which would not make more sugar available to stems, but the panicle had much lower ^{11}C partitioning in the dwarf sweet sorghum than the grain sorghum, which is consistent with the "competing sink" model. Although reduced sink strength of the panicle may contribute, sugar accumulation likely is not simply a function of reduced photoassimilate demand by the seedhead. Indeed, sugar accumulation does not correlate tightly with grain yield (Gutjahr et al. 2013), and some sweet sorghum varieties that accumulate a high sugar concentration in the stem also develop a moderately large panicle (Rutto et al. 2013). Removal of the reproductive sink of sweet sorghum plants (i.e., by removing the panicle, or by comparing near isogenic fertile and sterile lines)

does not necessarily alter the sugar concentrations in the stem, particularly for varieties that accumulate sugars in the stem prior to anthesis (Fortmeier and Schubert 1995; Gutjahr et al. 2013). Also, there are substantial QTLs for sugar accumulation that do not colocalize with QTLs for grain yield (Murray et al. 2008). These data suggest that lower demand for carbon in the panicle does not fully account for the increased partitioning of sugars to sweet sorghum stems.

Since sugar uptake into storage tissues is not a passive process, it is likely that accumulation of high sugar concentrations requires stems with high sink demand. Sink demand is largely controlled by the capacity of the sink for phloem unloading, which in turn may be limited by the capacity of the sink tissue for storage and/or utilization of carbohydrates (Arnold and Schultz 2002; Viola et al. 2001; Bihmidine et al. 2013). In sugar-accumulating sweet sorghum stems, sucrose is both the primary transport form and storage form of carbon. Sucrose is unloaded apoplastically and stored in stem parenchyma cells, which are symplastically isolated from the phloem (Bihmidine et al. 2015). However, this pathway is not universal, and sugarcane stems have been reported to unload sucrose from the phloem symplastically into storage

parenchyma cells, and then store the sucrose in the vacuoles and the surrounding apoplast (see Bihmidine et al., 2013 for discussion). In sweet sorghum stems, unlike the apoplastic unloading that occurs in many growing tissues, the majority of sucrose is not hydrolyzed by cell wall invertases, taken up as hexoses, and then reassembled inside the storage cells (Hoffmann-Thoma et al. 1996; Qazi et al. 2012; Tarpley et al. 1994; Tarpley and Vietor 2007). Rather, sucrose is unloaded and transferred to the storage cells as intact sucrose (Tarpley and Vietor 2007; Bihmidine et al. 2013).

Uptake of sucrose from the apoplast to stem parenchyma cells is likely mediated by one or more SUTs (Bihmidine et al. 2015). Higher expression in sweet dwarf sorghum than grain sorghum suggests that SbSUT1, SbSUT4, and SbSUT6 could be involved in sugar accumulation in middle internodes, perhaps through direct uptake into storage parenchyma cells. Previous reports on expression of SUTs found similar tissue expression patterns, but each found slightly different patterns of differential SUT expression between various sweet and grain sorghum cultivars (Bihmidine et al. 2015; Milne et al. 2013; Qazi et al. 2012). Comparing middle internodes across studies, SUT1 and SUT2 were expressed at high levels, SUT3 was not expressed, and SUT5 and SUT6 were expressed at relatively low levels both here and in previous studies (Bihmidine et al. 2015; Milne et al. 2013; Qazi et al. 2012). SUT4 expression was lower than SUT1 and SUT2 here and in Bihmidine et al. (2015), but was close to SUT1 and SUT2 expression levels reported by Qazi et al. (2012) and Milne et al. (2013). In all of the previous studies, comparison between grain and tall sweet sorghum varieties required either comparison of different developmental stages, or sampling of tissues at different times (e.g., 37 days between sampling of internodes from grain and sweet sorghum varieties in Milne et al. 2013). Thus, either developmental differences or environmental differences between grain and sweet sorghum plants may explain some of the variability among the different studies. In the present study, because we selected sweet and grain sorghum lines with similar timing of development, internode tissues for qPCR were sampled at the same time and the same developmental stage for both sweet and grain sorghums. Recently, Milne et al. (2017) suggested that SbSUT1 and SbSUT5 are involved in sucrose uptake to storage parenchyma cells in sweet sorghum stems, based on developmental expression patterns and localization. SUTs function as proton:sucrose symporters and use the energy stored in the proton motive force across the plasma membrane to move sucrose up its concentration gradient (Lalonde et al. 2004; Sauer 2007; Sivitz et al. 2005). Our data showing upregulation of SbSUT1 in dwarf sweet sorghum internodes support a role for SbSUT1 in taking up sugars into cells in maturing stems, potentially directly into storage parenchyma cells, although other cell types are also possible (Bihmidine et al. 2013).

In addition, a possible regulatory role was suggested for SbSUT2 (SbSUT4 by Milne's nomenclature) in the release of sucrose from vacuoles in storage parenchyma cells during internode elongation (Milne et al. 2017). Consistent with this finding, in our study SbSUT2 was upregulated only in upper internodes of sweet dwarf sorghum, which did not accumulate sugars relative to grain sorghum. It has been proposed that sucrose is leaked from phloem by a SWEET channel, pumped into storage parenchyma cells by SUTs, and then pumped into vacuoles by tonoplast sugar transporters (TSTs) (Bihmidine et al. 2015, 2016). Multiple QTLs relating to sugar accumulation have been localized near several SUT, SWEET, and TST genes (Bian et al. 2006; Felderhoff et al. 2012; Guan et al. 2011; Murray et al. 2009; Shiringani et al. 2010). It is possible that the rate-limiting step of stem sugar accumulation may be dynamic, such that SUTs are the rate-limiting step some of the time but not always. Future work will be necessary to resolve the roles of SUTs and other sugar transporters in sweet sorghum stems.

The transient accumulation of carbohydrates in grain crops such as grain sorghum and wheat, suggests that export from leaves increases before the sink demand increases in reproductive structures, but it is not clear what purpose this offset in timing serves. It has been suggested that these carbohydrates stored in stems, when remobilized, may give a transient boost to the supply of carbon and energy for the growth of reproductive structures (Scofield et al. 2009). However, we observed here that the partitioning of recently fixed carbon from leaves to the reproductive structures can be quite high in grain sorghum (i.e., 30% of all assimilated ^{11}C), which suggests that leaves have ample capacity to supply carbon and energy directly, rather than through a transient storage pool. Increased sugar export from leaves serves as a signal promoting flower development (Wang et al. 2021). Perhaps, the sugar accumulation in stems that occurred concomitant with increased export from leaves in sorghum may play a role in the vegetative-to-reproductive phase transition. Alteration of sugar signaling pathways could result in both the reduced seedhead growth and the increased accumulation of sugar in stems that occur in sweet sorghum. The differential expression of sugar-responsive genes that we observed between grain and sweet dwarf sorghum lends some support to this hypothesis.

Overall, identifying a mechanism for reduced photoassimilate demand in the panicle may present a possible avenue to enhance photoassimilate availability to sugar accumulating stems, but recent studies indicate that tradeoffs between seed yield and stem sugar yield are not straight forward. Our results indicate that future research should focus on phloem unloading in the stem, not on photosynthesis in or export of carbon from leaves, to identify the mechanism driving sugar accumulation in sweet sorghum stems. Understanding this phloem unloading mechanism may lead to an effective

approach to further enhance sugar accumulation in sweet sorghum stems, or to develop this trait in other crop species.

References

Arnold TM, Schultz JC (2002) Induced sink strength as a prerequisite for induced tannin biosynthesis in developing leaves of *Populus*. Oecologia 130:585–593

Babst BA, Karve AA, Judt T (2013) Radio-metabolite analysis of carbon-11 biochemical partitioning to nonstructural carbohydrates for integrated metabolism and transport studies. Plant Cell Physiol 54(6):1016–1025. https://doi.org/10.1093/pcp/pct045

Baker RF, Leach KA, Boyer NR, Swyers MJ, Benitez-Alfonso Y, Skopelitis T, Luo A, Sylvester A, Jackson D, Braun DM (2016) Sucrose transporter *ZmSut1* expression and localization uncover new insights into sucrose phloem loading. Plant Physiol 172(3):1876–1898. https://doi.org/10.1104/pp.16.00884

Bezrutczyk M, Hartwig T, Horschman M, Char SN, Yang J, Yang B, Frommer WB, Sosso D (2018) Impaired phloem loading in *zmsweet13a, b,* c sucrose transporter triple knock-out mutants i*n Zea ma*ys. New Phytol 218(2):594–603. https://doi.org/10.1111/nph.15021

Bian Y-l, Yazaki S, Inoue M, Cai H-w (2006) QTLs for sugar content of stalk in sweet sorghum (*Sorghum bicolor* L. Moench). Agric Sci China 5(10):736–744. https://doi.org/10.1016/S1671-2927(06)60118-1

Bihmidine S, Hunter CTI, Johns CE, Koch KE, Braun DM (2013) Regulation of assimilate import into sink organs: update on molecular drivers of sink strength. Front Plant Sci 4:177. https://doi.org/10.3389/fpls.2013.00177

Bihmidine S, Baker RF, Hoffner C, Braun DM (2015) Sucrose accumulation in sweet sorghum stems occurs by apoplasmic phloem unloading and does not involve differential sucrose transporter expression. BMC Plant Biol 15(1):1–22. https://doi.org/10.1186/s12870-015-0572-8

Bihmidine S, Julius BT, Dweikat I, Braun DM (2016) Tonoplast sugar transporters (SbTSTs) putatively control sucrose accumulation in sweet sorghum stems. Plant Signal Behav 11(1):e1117721. https://doi.org/10.1080/15592324.2015.1117721

Bryan WL (1990) Solid-state fermentation of sugars in sweet sorghum. Enzyme Microb Technol 12(6):437–442

Calvino M, Messing J (2012) Sweet sorghum as a model system for bioenergy crops. Curr Opin Biotechnol 23(3):323–329. https://doi.org/10.1016/j.copbio.2011.12.002

Dweikat I, Weil C, Moose S, Kochian L, Mosier N, Ileleji K, Brown P, Peer W, Murphy A, Taheripour F, McCann M, Carpita N (2012) Envisioning the transition to a next-generation biofuels industry in the US Midwest. Biofuel Bioprod Bior 6(4):376–386. https://doi.org/10.1002/bbb.1342

Felderhoff TJ, Murray SC, Klein PE, Sharma A, Hamblin MT, Kresovich S, Vermerris W, Rooney WL (2012) QTLs for energy-related traits in a sweet × grain sorghum [*Sorghum bicolor* (L.) Moench] mapping population. Crop Sci 52(5):2040–2049. https://doi.org/10.2135/cropsci2011.11.0618

Ferrieri RA, Wolf AP (1983) The chemistry of positron emitting nucleogenic atoms with regard to preparation of labeled compounds of practical utility. Radiochim Acta 34:69–83

Fortmeier R, Schubert S (1995) Storage of non-structural carbohydrates in sweet sorghum [*Sorghum bicolor* (L.) Moench]: comparison of sterile and fertile lines. J Agron Crop Sci 175(3):189–193. https://doi.org/10.1111/j.1439-037X.1995.tb00210.x

Gelli M, Mitchell SE, Liu K, Clemente TE, Weeks DP, Zhang C, Holding DR, Dweikat IM (2016) Mapping QTLs and association of differentially expressed gene transcripts for multiple agronomic traits under different nitrogen levels in sorghum. BMC Plant Biol 16(1):16. https://doi.org/10.1186/s12870-015-0696-x

Gorz HJ, Haskins FA, Johnson BE (1990) Registration of 15 germplasm lines of grain sorghum and sweet sorghum. Crop Sci 30(3):762–763. https://doi.org/10.2135/cropsci1990.0011183X003000030089x

Guan Y-a, Wang H-l, Qin L, Zhang H-w, Yang Y-b, Gao F-j, Li R-y, Wang H-g (2011) QTL mapping of bio-energy related traits in Sorghum. Euphytica 182(3):431. https://doi.org/10.1007/s10681-011-0528-5

Gutjahr S, Vaksmann M, Dingkuhn M, Thera K, Trouche G, Braconnier S, Luquet D (2013) Grain, sugar and biomass accumulation in tropical sorghums. I. Trade-offs and effects of phenological plasticity. Funct Plant Biol 40(4):342–354. https://doi.org/10.1071/FP12269

Hoffmann-Thoma G, Hinkel K, Nicolay P, Willenbrink J (1996) Sucrose accumulation in sweet sorghum stem internodes in relation to growth. Physiol Plant 97(2):277–284. https://doi.org/10.1034/j.1399-3054.1996.970210.x

Karve A, Alexoff D, Kim D, Schueller M, Ferrieri R, Babst BA (2015) *In vivo* quantitative imaging of photoassimilate transport dynamics and allocation in large plants using a commercial positron emission tomography (PET) scanner. BMC Plant Biol 15(1):273. https://doi.org/10.1186/s12870-015-0658-3

Kim D, Alexoff DL, Schueller M, Babst B, Ferrieri R, Fowler JS, Schlyer DJ (2014) The design and performance of a portable handheld ¹¹CO₂ delivery system. Appl Radiat Isot 94:338–343. https://doi.org/10.1016/j.apradiso.2014.09.008

Knoblauch M, Peters WS (2010) Munch, morphology, microfluidics—our structural problem with the phloem. Plant, Cell Environ 33(9):1439–1452. https://doi.org/10.1111/j.1365-3040.2010.02177.x

Lacointe A, Minchin PEH (2008) Modelling phloem and xylem transport within a complex architecture. Funct Plant Biol 35:772–780

Lalonde S, Wipf D, Frommer WB (2004) Transport mechanisms for organic forms of carbon and nitrogen between source and sink. Annu Rev Plant Biol 55:341–372

Loening AM, Gambhir SS (2003) AMIDE: a free software tool for multi-modality medical image analysis. Mol Imaging 2(3):131–137

Lohaus G, Hussmann M, Pennewiss K, Schneider H, Zhu J-J, Sattelmacher B (2000) Solute balance of a maize (*Zea mays* L.) source leaf as affected by salt treatment with special emphasis on phloem retranslocation and ion leaching. J Exp Bot 51(351):1721–1732. https://doi.org/10.1093/jexbot/51.351.1721

McCormick AJ, Cramer MD, Watt DA (2006) Sink strength regulates photosynthesis in sugarcane. New Phytol 171:759–770. https://doi.org/10.1111/j.1469-8137.2006.01785.x

McCormick AJ, Cramer MD, Watt DA (2008) Changes in photosynthetic rates and gene expression of leaves during a source-sink perturbation in sugarcane. Ann Bot 101:89–102. https://doi.org/10.1093/aob/mcm258

Milne RJ, Byrt CS, Patrick JW, Grof CPL (2013) Are sucrose transporter expression profiles linked with patterns of biomass partitioning in *Sorghum* phenotypes? Front Plant Sci. https://doi.org/10.3389/fpls.2013.00223

Milne RJ, Perroux JM, Rae AL, Reinders A, Ward JM, Offler CE, Patrick JW, Grof CPL (2017) Sucrose transporter localization and function in phloem unloading in developing stems. Plant Physiol 173(2):1330–1341. https://doi.org/10.1104/pp.16.01594

Minchin PEH (2007) Mechanistic modelling of carbon partitioning. In: Vos J, Marcelis LFM, De Visser PHB, Struik PC, Evers JB (eds) Functional-structural plant modelling in crop production, vol 22. Wageningen UR Frontis Series. Springer, Dordrecht, pp 113–122

Murray SC, Sharma A, Rooney WL, Klein PE, Mullet JE, Mitchell SE, Kresovich S (2008) Genetic improvement of sorghum as a biofuel feedstock: I. QTL for stem sugar and grain nonstructural carbohydrates. Crop Sci 48(6):2165–2179. https://doi.org/10.2135/cropsci2008.01.0016

Murray SC, Rooney WL, Hamblin MT, Mitchell SE, Kresovich S (2009) Sweet sorghum genetic diversity and association mapping for brix and height. Plant Genome. https://doi.org/10.3835/plantgenome2008.10.0011

Nabity PD, Zavala JA, Delucia EH (2009) Indirect suppression of photosynthesis on individual leaves by arthropod herbivory. Ann Bot 103(4):655–663. https://doi.org/10.1093/aob/mcn127

Ohshima T, Hayashi H, Chino M (1990) Collection and chemical composition of pure phloem sap from *Zea mays* L. Plant Cell Physiol 31(5):735–737

Olson SN, Ritter K, Medley J, Wilson T, Rooney WL, Mullet JE (2013) Energy sorghum hybrids: functional dynamics of high nitrogen use efficiency. Biomass Bioenerg 56:307–316. https://doi.org/10.1016/j.biombioe.2013.04.028

Papini-Terzi FS, Rocha FR, Vêncio RVN, Felix JM, Branco DS, Waclawovsky AJ, Del Bem LEV, Lembke CG, Costa MDL, Nishiyama MY, Vicentini R, Vincentz MGA, Ulian EC, Menossi M, Souza GM (2009) Sugarcane genes associated with sucrose content. BMC Genomics 10:120. https://doi.org/10.1186/1471-2164-10-120

Patrick JW (2013) Does Don Fisher's high-pressure manifold model account for phloem transport and resource partitioning? Front Plant Sci. https://doi.org/10.3389/fpls.2013.00184

Pfaffl MW (2001) A new mathematical model for relative quantification in real-time RT–PCR. Nucleic Acids Res 29(9):e45. https://doi.org/10.1093/nar/29.9.e45

Prasad S, Singh A, Jain N, Joshi HC (2007) Ethanol production from sweet sorghum syrup for utilization as automotive fuel in India. Energy Fuels 21(4):2415–2420. https://doi.org/10.1021/ef060328z

Qazi HA, Paranjpe S, Bhargava S (2012) Stem sugar accumulation in sweet sorghum—activity and expression of sucrose metabolizing enzymes and sucrose transporters. J Plant Physiol 169:605–613. https://doi.org/10.1016/j.jplph.2012.01.005

Rennie EA, Turgeon R (2009) A comprehensive picture of phloem loading strategies. Proc Natl Acad Sci USA 106(33):14162–14167. https://doi.org/10.1073/pnas.0902279106

Rooney WL, Blumenthal J, Bean B, Mullet JE (2007) Designing sorghum as a dedicated bioenergy feedstock. Biofuel Bioprod Bior 1(2):147–157. https://doi.org/10.1002/bbb.15

Ross-Elliott TJ, Jensen KH, Haaning KS, Wager BM, Knoblauch J, Howell AH, Mullendore DL, Monteith AG, Paultre D, Yan D, Otero-Perez S, Bourdon M, Sager R, Lee J-Y, Helariutta Y, Knoblauch M, Oparka KJ (2017) Phloem unloading in *Arabidopsis* roots is convective and regulated by the phloem-pole pericycle. Elife 6:e24125. https://doi.org/10.7554/eLife.24125

Rozen S, Skaletsky H (1999) Primer3 on the WWW for general users and for biologist programmers. In: Misener S, Krawetz SA (eds) Bioinformatics methods and protocols. Humana Press, Totowa, NJ, pp 365–386. https://doi.org/10.1385/1-59259-192-2:365

Rutto LK, Xu Y, Brandt M, Ren S, Kering MK (2013) Juice, ethanol, and grain yield potential of five sweet sorghum (*Sorghum bicolor* [L.] Moench) cultivars. J Sustain Bioenerg Syst 3(2):113–118. https://doi.org/10.4236/jsbs.2013.32016

Sauer N (2007) Molecular physiology of higher plant sucrose transporters. FEBS Lett 581(12):2309–2317. https://doi.org/10.1016/j.febslet.2007.03.048

Scofield GN, Ruuska SA, Aoki N, Lewis DC, Tabe LM, Jenkins CLD (2009) Starch storage in the stems of wheat plants: localization and temporal changes. Ann Bot 103:859–868. https://doi.org/10.1093/aob/mcp010

Shiringani AL, Frisch M, Friedt W (2010) Genetic mapping of QTLs for sugar-related traits in a RIL population of *Sorghum bicolor* L. Moench Theor Appl Genet. https://doi.org/10.1007/s00122-010-1312-y

Sivitz AB, Reinders A, Ward JM (2005) Analysis of the transport activity of barley sucrose transporter HvSUT1. Plant Cell Physiol 46(10):1666–1673. https://doi.org/10.1093/pcp/pci182

Slewinski TL, Braun DM (2010) Current perspectives on the regulation of whole-plant carbohydrate partitioning. Plant Sci 178:341–349. https://doi.org/10.1016/j.plantsci.2010.01.010

Slewinski TL, Garg A, Johal GS, Braun DM (2010) Maize SUT1 functions in phloem loading. Plant Signal Behav 5(6):687–690

Slewinski TL, Meeley R, Braun DM (2009) *Sucrose transporter1* functions in phloem loading in maize leaves. J Exp Bot 60(3):881–892. https://doi.org/10.1093/jxb/ern335

Tarpley L, Lingle SE, Vietor DM, Andrews DL, Miller FR (1994) Enzymatic control of nonstructural carbohydrate concentrations in stems and panicles of sorghum. Crop Sci 34(2):446–452

Tarpley L, Vietor DM (2007) Compartmentation of sucrose during radial transfer in mature sorghum culm. BMC Plant Biol 7:33. https://doi.org/10.1186/1471-2229-7-33

Vietor DM, Miller FR (1990) Assimilation, partitioning, and nonstructural carbohydrates in sweet compared with grain sorghum. Crop Sci 30(5):1109–1115. https://doi.org/10.2135/cropsci1990.0011183X003000050030x

Viola R, Roberts AG, Haupt S, Gazzani S, Hancock RD, Marmiroli N, Machray GC, Oparka KJ (2001) Tuberization in potato involves a switch from apoplastic to symplastic phloem unloading. Plant Cell 13(2):385–398. https://doi.org/10.1105/tpc.13.2.385

Wang M, Le Gourrierec J, Jiao F, Demotes-Mainard S, Perez-Garcia M-D, Ogé L, Hamama L, Crespel L, Bertheloot J, Chen J, Grappin P, Sakr S (2021) Convergence and divergence of sugar and cytokinin signaling in plant development. Int J Mol Sci 22(3):1282

Weiner H, Blechschmidt-Schneider S, Mohme H, Eschrich W, Heldt HW (1991) Phloem transport of amino-acids. Comparison of amino-acid contents of maize leaves and of the sieve tube exudate. Plant Physiol Biochem 29(1):19–23